PRELIMINARY GEOCHEMICAL DATA OF THE MAFIC ROCKS FROM THE OVACIK AND PÜLÜMÜR OPHIOLITE ZONE (EASTERN ANATOLIA, TURKEY): IMPLICATIONS FOR THE GEODYNAMIC EVOLUTION OF THE NORTHERN NEOTETHYAN OCEAN

Okay Çimen*,✉ and **Ayten Öztüfekçi Önal***

* *Department of Geological Engineering, Munzur University Tunceli, Turkey.*
✉ *Corresponding author, email: okaycimen@gmail.com*

ABSTRACT

The İzmir-Ankara-Erzincan-Sevan-Akera Suture Belt (IAESASB) stretches from the Aegean Sea to the Lesser Caucasus and includes the remnants of the Northern Neotethys. The Ovacık and Pülümür Ophiolite Zone (OPOZ) to the north of Tunceli is less-known members of this belt. In this study, preliminary geochemical data from the basaltic and gabbroic rocks from this zone are presented to provide the first insights into their geochemistry. The studied mafic samples exhibit geochemical characteristics of an intra-oceanic subduction system. Three types of samples were differentiated on the basis of their major, trace and rare earth element (REE) geochemistry. The first one is boninitic and displays highly depleted elemental pattern (relative to N-MORB) and concave REE profile. The second type is akin to back-arc basin basalts (BABB) and generally reflects normal-MORB (NMORB)-like high field strength element (HFSE) patterns coupled with negative Nb anomalies. The last type is relatively similar to the BABB-type, but it lacks the marked negative anomaly in Nb and can be ascribed to the mid-ocean ridge basalt (MORB). The overall geochemical features suggest that these mafic rocks were predominantly generated in a supra-subduction setting from a subduction-modified mantle source. It is further suggested that the Ovacık and Pülümür Ophiolite Zone was formed in an oceanic arc-basin system within the northward subducting Northern Neotethys.

INTRODUCTION

According to the commonly accepted view, a number of terranes or continental micro-plates were amalgamated during the closure of the Neotethyan oceanic branches (e.g., Şengör and Yılmaz, 1981; Göncüoğlu et al., 1997; Robertson et al., 2014). In the Anatolian realm, these oceanic branches which comprise ophiolites and mélanges are represented from north to south by the Intra-Pontide Suture (IPS; Catanzariti et al., 2013; Göncüoğlu et al., 2014; Marroni et al., 2014; Ellero et al., 2015; Frassi et al., 2016; Çimen et al., 2016a; 2017) between the İstanbul-Zonguldak Terrane (IZT) and the Sakarya Composite Terrane (SCT), the Izmir-Ankara-Erzincan-Sevan-Akera Suture Belt (IAESASB; Aldanmaz et al., 2008; Parlak et al., 2013; Topuz et al., 2013; Robertson et al., 2014; Uysal et al., 2015) between the SCT and the Tauride-Anatolide Platform (TAP), the southern branch of Neotethyan (Robertson, 2002; Bağcı et al., 2006; 2008; Uysal et al., 2007; Yılmaz and Yılmaz, 2013; Akmaz et al., 2014; Parlak, 2016) between the TAP and the Arabian Platform.

In particular, the IAESASB stretches from the Aegean Sea to the Lesser Caucasus and includes the remnants of the northern Neotethys (Fig. 1a). These ophiolites have been derived from a subduction-accretion system during the closure of the Neotethyan ocean (Şengör and Yılmaz, 1981; Okay and Şahintürk, 1997; Çimen et al., 2016b). Their ages range from Late Jurassic to Early Cretaceous (Dilek and Thy, 2006; Topuz et al., 2013), whereas the formation of the mélange complexes were assigned to Late Cretaceous (Parlak et al., 2013; Robertson et al., 2014). The geochemical characteristics of the ophiolites suggest various tectonic setting such as mid-ocean ridge, oceanic island and island arc (e.g., Yalınız et al., 2000; Göncüoğlu et al., 2006; Aldanmaz et al., 2008; Parlak et al., 2013). Their emplacement onto the Tauride-Anatolide margin started as early as Maastrichtian and lasts until Early Eocene (Şengör and Yılmaz, 1981; Yılmaz et al., 1997; Floyd et al., 2000; Göncüoğlu et al., 2000).

Similar Tethyan ophiolites (Fig. 1a) of Early-Middle Jurassic age occur further east in Armenia (Galoyan et al., 2009; Rolland et al., 2010; Hässig et al., 2013). Moreover, the geochemical characteristics of magmatic rocks indicate variable affinities from tholeiitic to calc-alkaline and alkaline (Knipper and Khain, 1980; Knipper et al, 1986). In contrast to the better-known Izmir-Ankara segment (e.g., Floyd, 1993; Önen and Hall, 1993; Göncüoğlu et al., 2000; Göncüoğlu et al., 2006; Bortolotti et al., 2013) and Ankara-Erzincan (e.g., Okay and Şahintürk, l997; Dilek and Thy, 2006; Rice et al., 2006, Eyüboğlu et al., 2007; Çelik et al., 2011; Topuz et al., 2013) segments, the Ovacık-Pülümür ophiolites are the least-known members of this suture belt (Çimen et al., 2016b). The ophiolitic assemblages of the Ovacık-Pülümür segment forms approximately a 90 km long and 20 km wide zone (Fig. 1b), named as Ovacık-Pülümür Ophiolite Zone (OPOZ) in this study. At its northeastern edge, it is dissected by the North Anatolian Fault and separated from the main Izmir-Ankara-Erzincan Suture Belt by the intervening Munzur Carbonate Platform (MCP; a part of eastern Taurides).

Recently, Çimen et al. (2016b) reported the first petrological data on the OPOZ chromitites and mantle peridotites that indicate derivation from a intra-oceanic back-arc tectonic setting. However, no published geochemical or petrological data from the magmatic rocks within the OPOZ are available. Here, we present preliminary geochemical data from the basaltic and gabbroic rocks. Our goal is to give the first insights into their geochemistry and provide better understanding of the evolution of the northern branch of Neotethyan Ocean.
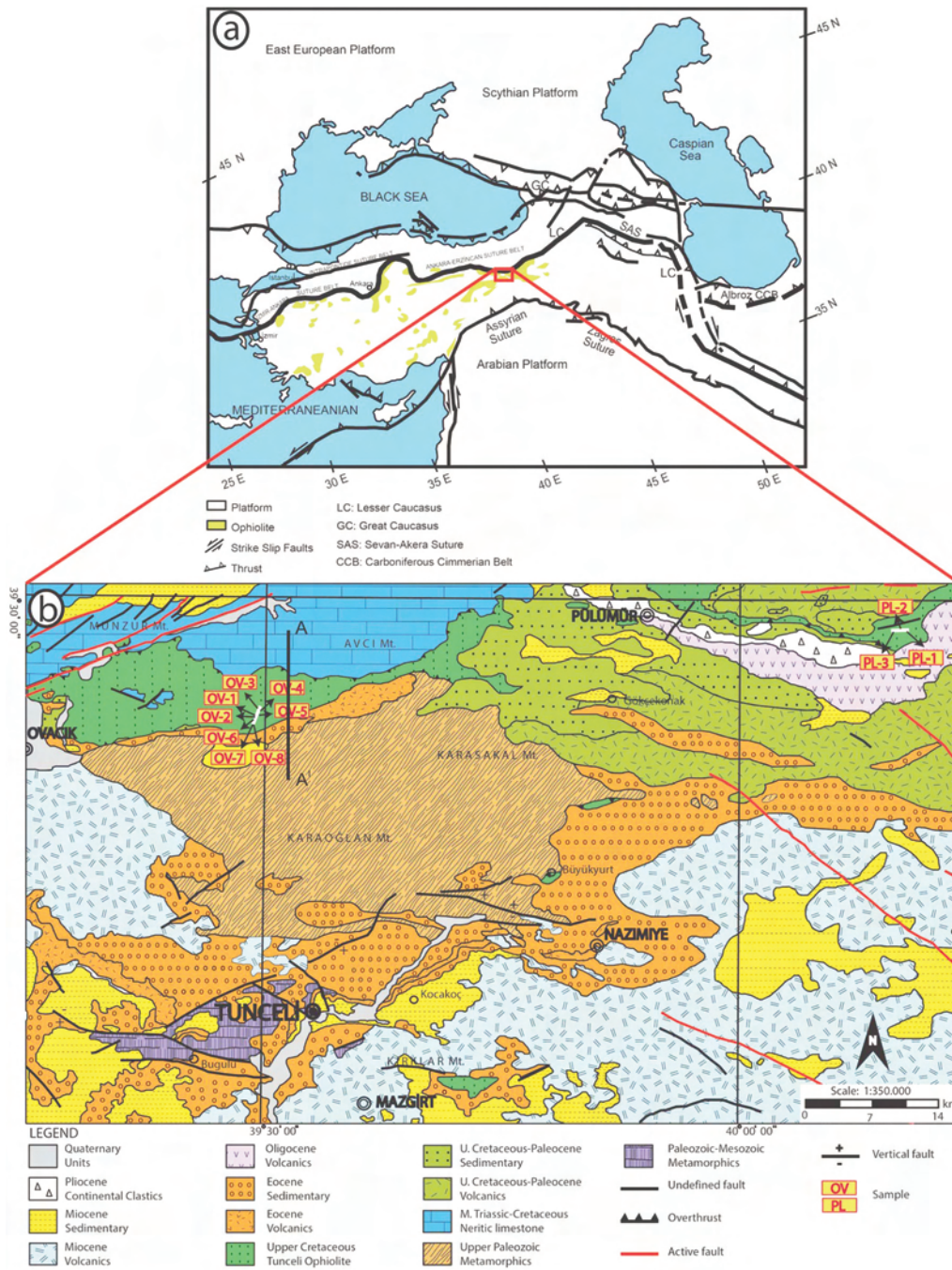
Fig. 1 - a) Location of the study area in the tectonic sketch map of Anatolia (modified from Göncüoğlu et al., 1997; Avagyan et al., 2005); b) Geological map of the study area (modified from MTA, 2008).

GEOLOGICAL SETTING

Regional geology

The oceanic assemblages and continental fragments in Anatolia are related to the Tethyan evolution of Turkey during the Paleozoic and Mesozoic periods. The OPOZ is a piece of eastern part of the İzmir-Ankara-Erzincan suture belt (Fig. 1b). The SCT and TAP, which have formed by rifting at different times in the northern edge of the Gondwana, are separated by this suture belt (Fig. 2a). Göncüoğlu et al. (1997) describes the SCT unit as "Composite Terrane" due to the presence in its basement of several pre-Alpine terranes which record signatures of the different geological events. This terrane comprises the Pre-Jurassic assemblages (Variscan Terranes and Cimmerian Terranes) and their Jurassic-Late Cretaceous cover units (Göncüoğlu, 2010).

On the other hand, the TAP is located in the south of SCT and represents the continental platform between the IAESASB to the north (Fig. 2a) and the southern branch of Neotethys to the south (Göncüoğlu, 2010). The TAP consists of two important regions such as the Anatolides and the Taurides. The Anatolides are the metamorphic northern margin of the TAP and have been mainly metamorphosed and deformed during the Late Cretaceous to Early Cenozoic due to the Alpine orogeny (Bozkurt and Oberhansli, 2001; Candan et al., 2005). The Taurides represent the southern part of the TAP and are composed of a Cambrian basement overlain by Paleozoic to Early Tertiary thrust sheets (Özgül, 1984; Okay, 2008; Candan et al., 2016).
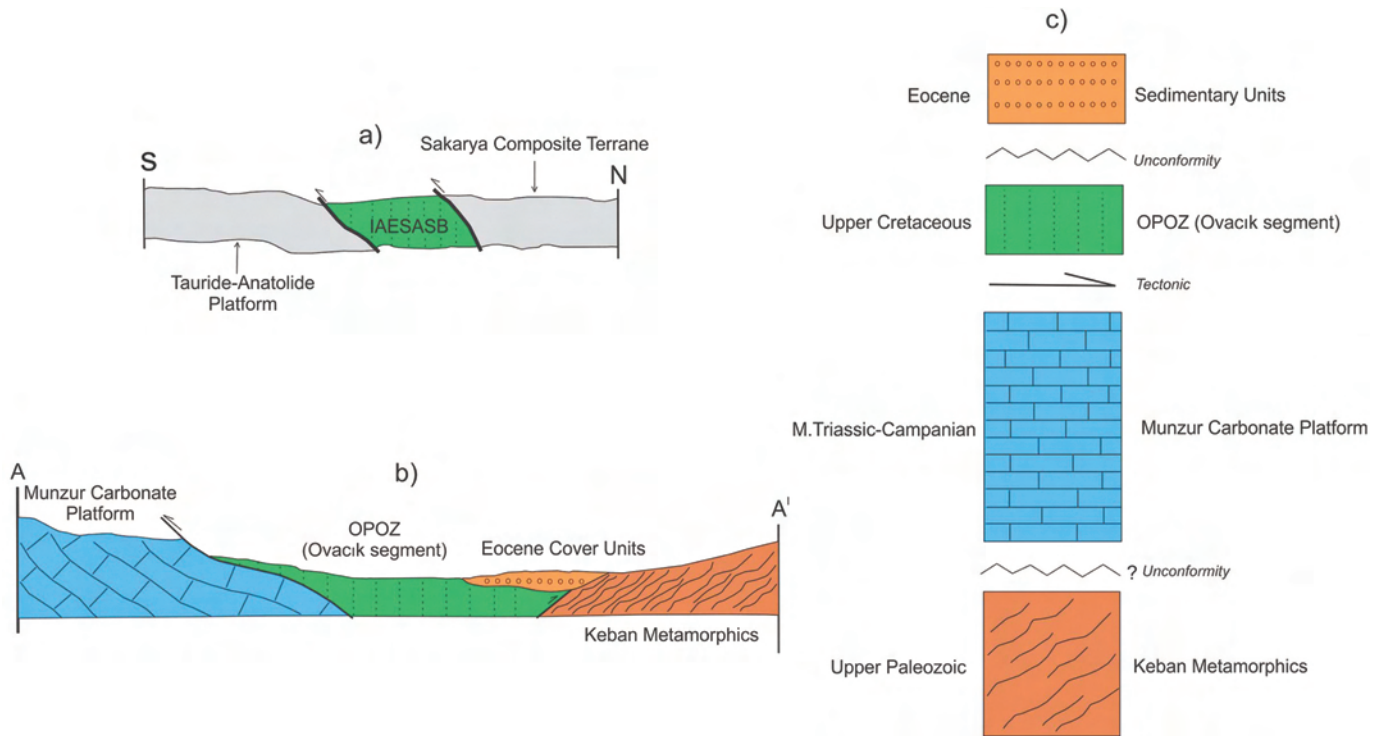
Fig. 2 - a) Sketch cross section between the Tauride-Anatolide Platform and Sakarya Composite Terrane (IAESASB: İzmir-Ankara-Erzincan-Sevan-Akera Suture Belt); b) Generalized geological cross-section of the study area (Ovacık Segment); c) Generalized stratigraphic column section of the study area (Ovacık segment).

Ovacık and Pülümür Ophiolite Zone (OPOZ)

In relation to the study area, the preliminary geological data has been reported by MTA (2008) and Çimen et al. (2016b). The basement rocks are composed of Late Paleozoic metamorphic rocks. They are tectonically overlain by the MCP and can be correlated with the upper stratigraphical section of the Keban Metamorphic Unit (KMU; Fig. 2b, c). The MCP, formed by continuous deposition during the Middle Triassic to Campanian, consists of algal biomicrites, calcarenites, pelagic limestones and reef limestone units (Fig. 2c; Özgül et al., 1981). The OPOZ tectonically overlies the basement rocks and the MCP in the north and northwest (Fig. 3a, b). The basement units and the OPOZ are unconformably covered by the Eocene sedimentary units in the Ovacık segment (Fig. 2b, c). Conversely, in the Pülümür segment, the OPOZ units are unconformably covered by the Oligocene volcanics and the Pliocene clastic sediments. The youngest geological unit is represented in the study area by the Quaternary alluviums that unconformably overlie all these units (Fig. 1b).

The OPOZ consists of a continuous sequence including ultramafic rocks (serpentinized peridotites), pillow lavas, sheeted dykes, gabbros, mudstones and limestone blocks (Fig. 3c, d). The mantle bodies are composed of dominant harburzgites with minor dunites, pyroxenites and chromite mineralizations (Fig. 3e, f). The peridotites show evidence of ductile to brittle deformations and are completely serpentinized (Çimen et al., 2016b). The magmatic rocks are mostly found in the western and eastern parts of the OPOZ (Fig. 1b). Some of the mudstones have been also affected by tectonic activities in the region as evidenced by folding structures (Fig. 3g, h).

PETROGRAPHY

The magmatic rocks from the OPOZ were grouped as basalts, diabases, and gabbros on the basis of their petrographic features. The basalts have generally aphanitic/microphaneritic and porphyritic texture (Fig. 4a). The phenocrysts are composed of plagioclase, orthopyroxene, clinopyroxene and subordinate olivine. In some cases, the plagioclase microliths exhibit flow texture by alignment to similar directions (Fig. 4a). The plagioclase phenocrysts commonly formed as subhedral to euhedral crystals. The other typical phenocryst phase is clinopyroxene that shows locally glomeroporphyritic texture (Fig. 4a). The orthopyroxene crystals are mostly euhedral and occasionally have plagioclase and opaque inclusions. The diabases consist of plagioclase and clinopyroxene. They are characterized by porphyritic texture. Subophitic texture can be seen by gathering large clinopyroxene minerals and plagioclase laths. The plagioclase phenocrysts have mostly subhedral shapes and display seriate texture by the presence of randomly oriented interlocking laths (Fig. 4b). Also epidote minerals can be observed as a secondary alteration product of the plagioclase. The clinopyroxene phenocrysts mostly formed as subhedral to anhedral crystals (Fig. 4b). Chloritization is observed at the edge parts of some clinopyroxene crystals. The mineral paragenesis of the gabbro generally includes olivine, clinopyroxene and plagioclase.
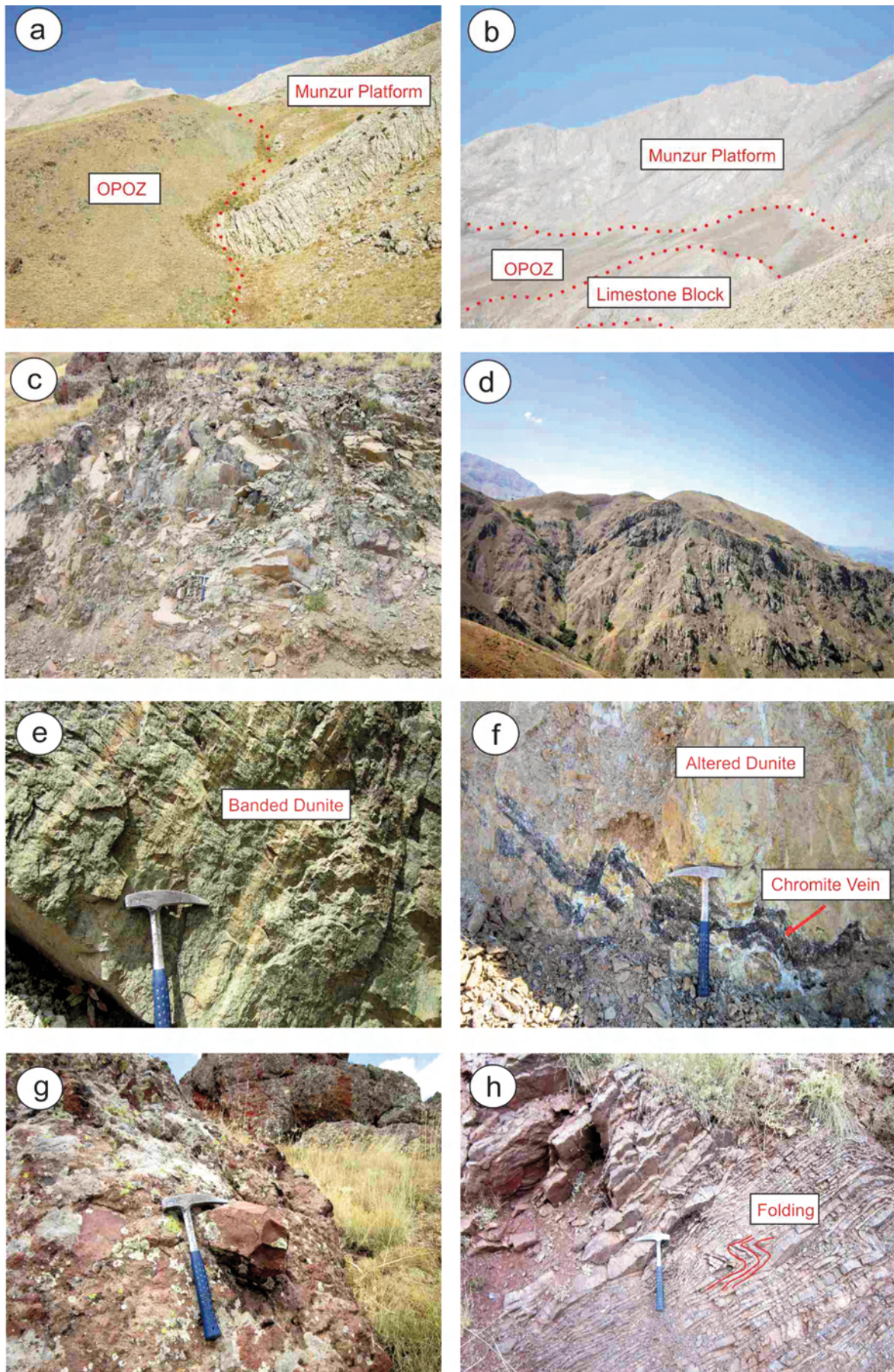
Fig. 3 - Field views of the units in the OPOZ: a, b) tectonic contact (thrust) between the OPOZ and Munzur Carbonate Platform; c, d) general view of the mafic rocks in the OPOZ; e) banded dunite ultramafic cumulate; f) chromite vein in an altered dunite; g) mudstone; h) folding in pelagic limestone-mudstone alternation with slump structures.
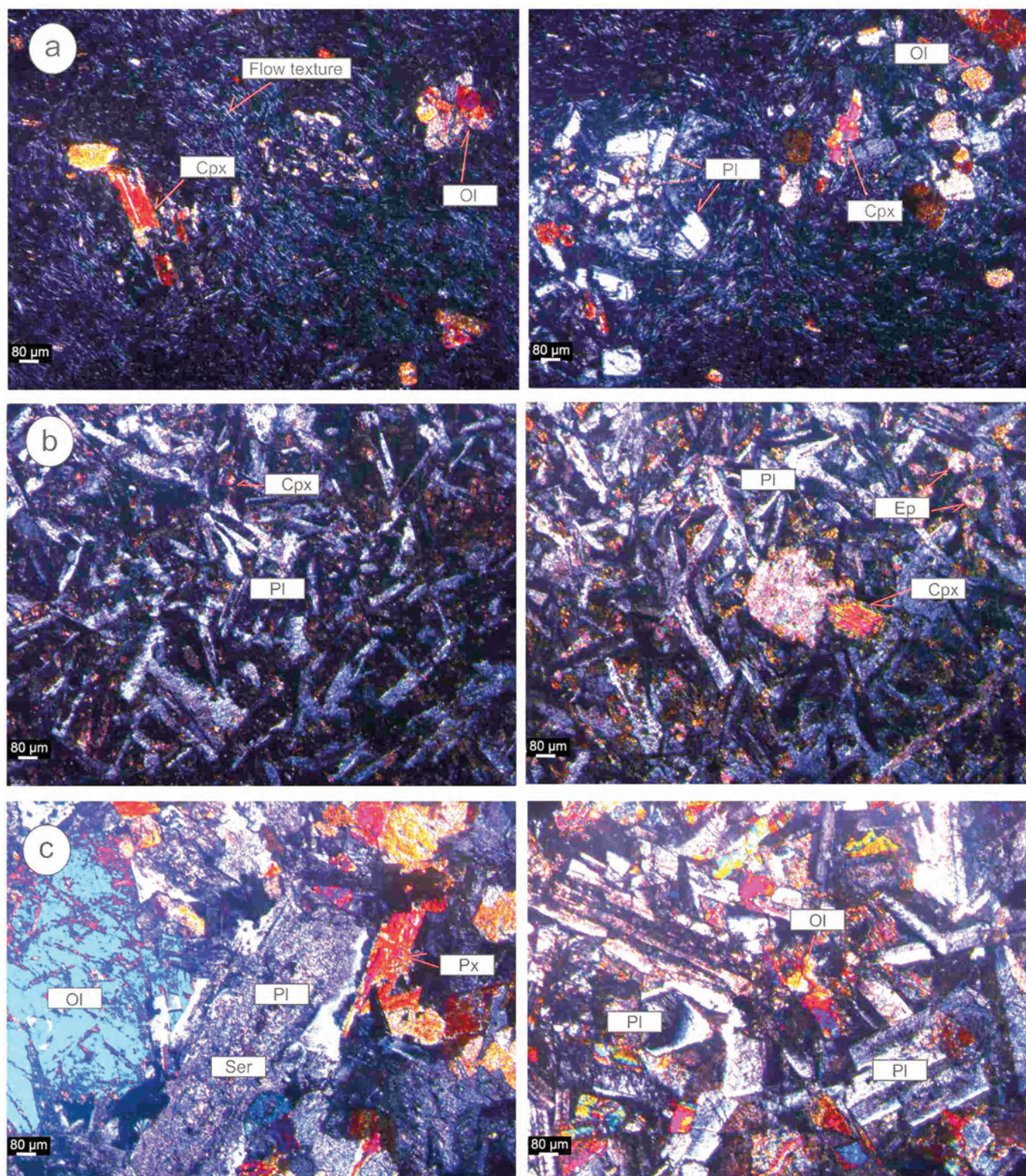
Fig. 4 - Thin section images of: a) mineral assemblages within the basalts; b) mineral paragenesis within the diabases; c) mineral assemblages within the gabbro (all images 4X, XPL- cross polarized light). Abbreviations: Ol- olivine, Cpx- clinopyroxene, Pl- plagioclase, Ep- epidote, Ser- sericitization).

The olivine phenocrysts are subhedral to euhedral and contain irregular fractures. They may be altered to iddingsite and chlorite. The plagioclase crystals are subhedral to euhedral and exhibit sericitization as alteration product (Fig. 4c). In some samples, the plagioclase phenocrysts show a seriate texture by the presence of randomly oriented interlocking laths (Fig. 4c). The clinopyroxene phenocrysts are clustered to display a glomeroporphyritic texture. Lastly, opaque minerals have been also observed and the cubic-shaped crystals may be magnetite and pyrite.

GEOCHEMISTRY

Analytical method

A total of eleven representative mafic magmatic rocks from the OPOZ were analyzed at the Acme Laboratories (Canada). Bulk rock major oxides and trace elements were analyzed using Inductively Coupled Plasma-Optical Emission Spectrometry (ICP-OES) and Inductively Coupled Plasma-Mass Spectrometry (ICP-MS) methods, respectively. The lithium metaborate/tetraborate fusion and dilute nitric digestion were performed for the total abundances of the major oxides and several minor elements. Loss on ignition (LOI) is determined by weight difference after ignition at 1000°C. In addition to these, the duplicates and standard reference materials were conducted during the analyses in order to ensure a measure of background noise, accuracy, and precision.

Post-magmatic alteration effects

The geochemical results were evaluated using Geochemical Data Toolkit (GCDkit) software (Janoušek et al., 2006) on the basis of the immobile element concentrations. The variable LOI values (2.1-5.3 wt%; Table 1) are consistent with the effects of hydrothermal alteration that has been evidenced by the petrographic studies (e.g., sericitization in plagioclase). The large ion lithophile elements (LILE; e.g., Ba, Rb and K_2O) display a scattered distribution due to the post-magmatic events (Fig. 5a) whereas the high field strength elemets (HFSE) and rare earth elements (REE) show good correlations because of their immobile characteristics during the alteration processes (Fig. 5b). The low MgO concentrations coupled with high LOI values of some

samples may result from alteration processes as well (see Table 1). Thus, the trace elements (Ti, Zr, rare earth elements, etc.) which have immobile characteristics under the alteration conditions (e.g.,, Pearce and Cann, 1973; Floyd and Winchester, 1978) have been considered for the geochemical evaluation. On the other hand, the LILEs have not been taken into account since they may behave mobile during the secondary alteration processes (Wood et al., 1976; Floyd et al., 2000). The gabbro samples were excluded from the classification diagrams based on immobile elements because they show a Fe-Ti oxide accumulation trend in the Mg# vs SiO_2/Al_2O_3 diagram (not reported; Montanini and Tribuzio, 2001) and are not representative of liquids.

Classification

The magmatic rocks from the OPOZ plot into the basalt field (Fig. 6) according to the classification diagram of Pearce (1996). However, three different rock groups belonging to different tectono-magmatic settings, such as fore-arc (boninitic), back arc basin basalts (BABB) and normal mid-ocean ridge basalt (N-MORB) have been geochemically identified based on the trace element systematics. Here, the Type 1 displays geochemical characteristics of boninitic rocks with higher SiO_2 (50.40 wt%) and MgO (8.70 wt%) concentrations and lower Zr/Ti (0.0029) values compared to the other samples (Table 1; Fig. 6). While the Type 2 has higher Zr/Ti (0.008-0.011) and lower Nb/Y (0.032-0.066) and MgO (2.87-6.90 wt%) values than the Type 1, the Type 3 has higher Zr/Ti (0.151), Nb/Y (0.100) values and lower SiO_2 (46.89 wt%) concentration than the other types (Table 1; Fig. 6).
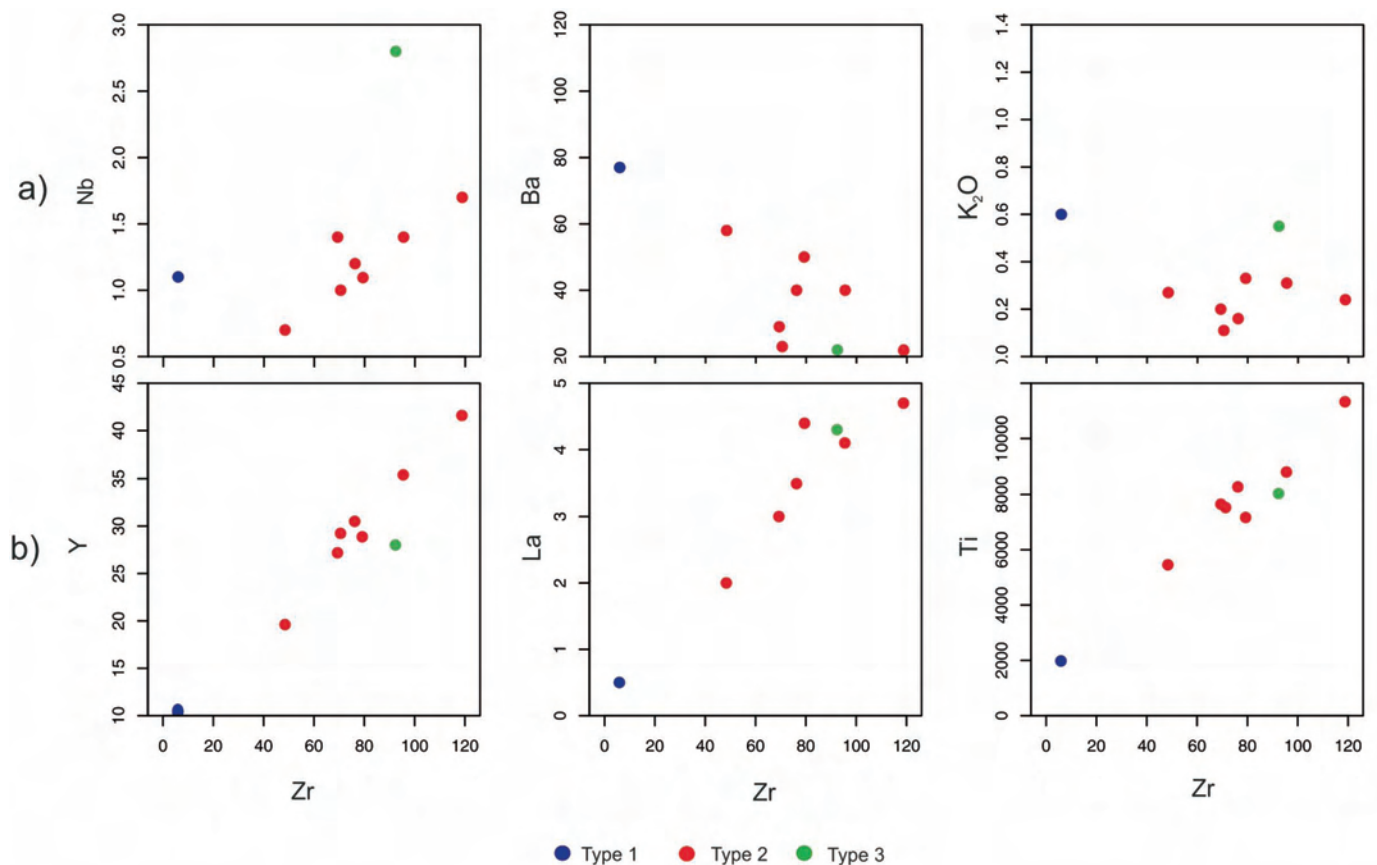

Fig. 5 - Plots of selected major and trace elements vs. Zr.

Table 1 - Major and trace element concentrations of the magmatic rocks from the OPOZ.

	Type 1	Type 2									Type 3
Sample	OV-3	OV-1	OV-2	OV-4	OV-5	OV-6	OV-7	PL-1	PL-2	PL-3	OV-8
Rock Type	Basalt	Diabase	Diabase	Basalt	Diabase	Basalt	Gabrro	Gabbro	Diabase	Diabase	Basalt
SiO_2 %	50.40	48.86	50.93	49.15	56.10	52.60	53.35	49.96	49.86	49.41	46.89
Al_2O_3	15.71	15.05	14.64	16.21	14.22	13.95	12.54	15.57	14.72	14.81	14.85
Fe_2O_3	8.76	11.72	11.50	11.18	10.16	8.81	11.30	10.11	11.54	9.63	10.46
MgO	8.70	6.90	4.34	5.14	4.34	2.97	2.87	6.62	5.16	5.59	6.59
CaO	5.97	7.45	7.44	8.28	7.24	10.82	9.49	9.04	10.61	12.87	11.28
Na_2O	4.22	3.39	5.46	2.87	3.05	3.59	3.17	3.49	4.13	3.31	3.39
K_2O	0.60	0.16	0.11	0.31	0.24	0.33	0.18	1.28	0.20	0.27	0.55
TiO_2	0.33	1.38	1.26	1.47	1.89	1.20	1.56	1.14	1.27	0.91	1.34
P_2O_5	0.02	0.11	0.12	0.15	0.15	0.10	0.12	0.10	0.10	0.05	0.15
MnO	0.13	0.22	0.90	0.15	0.17	0.16	0.16	0.16	0.18	0.15	0.17
Cr_2O_3	0.024	0.007	0.011	0.007	0.026	0.019	0.027	0.045	0.020	0.023	0.053
Ni *(ppm)*	52.5	20.4	21.3	36.2	20.7	16.5	14.8	41.8	16.7	14.4	79.4
Sc	39	35	33	37	32	24	25	35	34	35	38
LOI	5.0	4.6	3.2	4.8	2.3	5.3	5.0	2.3	2.1	2.8	4.1
Ba	77	40	23	40	21	50	104	62	29	58	22
Co	36.0	37.0	40.9	46.8	35.6	25.8	29.7	34.3	35.7	32.7	44.8
Cs	0.1	<0.1	<0.1	<0.1	0.2	<0.1	<0.1	3.7	3.0	0.2	0.3
Hf	0.3	2.3	2.3	3.0	3.3	2.0	2.5	1.8	2.1	1.3	2.5
Nb	1.1	1.2	1.0	1.4	1.7	1.1	1.1	1.7	1.4	0.7	2.8
Rb	7.7	3.6	1.4	2.9	5.6	4.6	1.7	48.2	3.7	5.1	9.4
Sr	272.7	318.6	110.1	405.8	149.3	192.8	775.0	494.4	230.8	306.8	336.1
Ta	<0.1	0.1	<0.1	0.1	<0.1	<0.1	<0.1	<0.1	0.1	<0.1	0.2
Th	<0.2	0.2	<0.2	<0.2	0.3	0.3	0.2	0.2	<0.2	<0.2	0.2
U	<0.1	0.4	<0.1	0.1	0.2	0.2	0.2	<0.1	<0.1	<0.1	<0.1
V	279	398	364	458	359	255	439	300	354	321	310
W	<0.5	<0.5	<0.5	<0.5	<0.5	<0.5	<0.5	<0.5	<0.5	<0.5	<0.5
Zr	5.9	76.2	70.5	95.5	118.8	79.2	93.2	70.4	69.3	48.4	92.4
Y	10.2	30.5	29.3	35.4	41.6	28.9	33.9	25.7	27.2	19.6	28
La	0.5	3.5	3.3	4.1	4.7	4.4	3.8	3.3	3.0	2.0	4.3
Ce	0.7	10.6	9.8	11.5	14.7	9.9	11.6	8.8	8.8	5.7	12.3
Pr	0.10	1.74	1.68	2.03	2.49	1.77	1.89	1.53	1.49	0.99	1.93
Nd	0.8	9.5	8.8	10.7	13.6	9.0	10.7	8.3	8.3	5.3	10.3
Sm	0.45	2.95	2.96	3.72	4.45	2.92	3.48	2.59	2.74	1.89	3.13
Eu	0.21	1.13	1.08	1.33	1.63	1.10	1.31	0.95	1.06	0.75	1.19
Gd	0.93	4.41	4.21	5.20	5.86	4.03	4.81	3.77	4.05	2.70	4.5
Tb	0.20	0.74	0.68	0.87	0.99	0.69	0.85	0.62	0.67	0.47	0.72
Dy	1.54	5.57	4.86	6.23	6.87	4.89	5.73	4.74	5.04	3.43	5.3
Ho	0.36	1.11	1.05	1.30	1.37	1.08	1.19	0.94	1.02	0.67	1.04
Er	1.09	3.01	2.87	3.74	3.90	3.11	3.47	2.56	2.91	1.90	2.87
Tm	0.18	0.48	0.42	0.54	0.58	0.44	0.50	0.39	0.43	0.43	0.29
Yb	1.15	2.95	2.58	3.13	3.69	2.79	3.16	2.41	2.49	2.77	1.87
Lu	0.20	0.48	0.42	0.49	0.57	0.44	0.55	0.36	0.42	0.42	0.30
Zr/Y	0.57	2.49	2.40	2.69	2.85	2.74	2.74	2.73	2.54	2.46	3.30
Nb/Y	0.10	0.03	0.03	0.03	0.04	0.38	0.03	0.06	0.05	0.03	0.10
Zr(M)	0.07	1.02	0.95	1.29	1.60	1.07	1.25	0.95	0.93	0.65	1.24
Zr/Nb	5.36	63.50	70.50	68.21	69.88	72.00	84.72	41.41	49.50	69.14	33.00
Sm/Yb	0.39	1.00	1.14	1.18	1.20	1.04	1.10	1.07	1.10	0.68	1.67
Dy/Yb	1.33	1.88	1.88	1.99	1.86	1.75	1.81	1.96	2.02	1.23	2.83
Mg#	46.13	33.67	24.55	28.39	26.92	22.52	17.97	36.09	27.83	33.36	35.20
Coordinates	4359632N	4359313N	4359335N	4359366N	4359370N	4359281N	4359085N	4369271N	4369432N	4369387N	4359090N
37 S	542172E	542075E	542080E	542299E	542300E	542062E	541828E	600156E	599829E	599708E	541835E

In relation to the multi-element diagrams, the Type 1 displays highly depleted HFSE concentrations relative to N-MORB (Nb = 1.1 ppm, Zr = 5.9 ppm; N-MORB Nb = 2.33 ppm, Zr = 74 ppm; Sun and McDonough, 1989) and is characterized by enrichments of the heavy rare earth elements (HREEs) relative to the middle rare earth elements (MREEs, $[Lu/Sm]_N$ = 2.74) and the light rare earth elements [LREEs; $(Lu/La)_N$ = 3.96; Fig. 7a]. Although the Type 2 exhibits highly depleted Nb (0.7-1.7 ppm) and slightly depleted Ti concentrations similar to the Type 1, it is enriched in the other HFSEs (e.g., Zr = 48.4-118.8 ppm). In addition, this type is also characterized by less fractionated REEs/chondrite-normalized patterns ($[La/Sm]_N$ = 0.98-1.42; Fig. 7b). The Type 3 is characterized by slightly depletions in Nb and Ti and displays more enriched patterns in terms of the HFSEs (Fig. 7c).
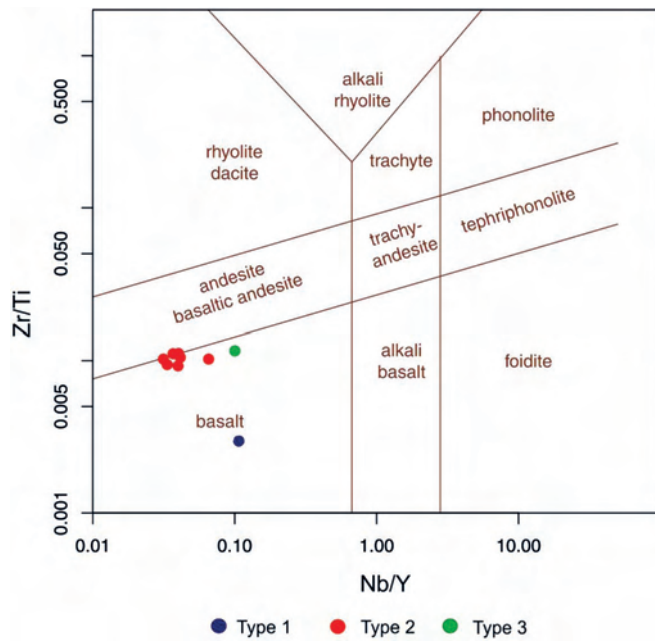
Fig. 6 - Zr-Ti vs. Nb-Y (after Pearce, 1996) diagram for the magmatic rocks from the OPOZ.

Mantle sources and geotectonic environments

The various spider and binary diagrams were used in order to put constraints on the mantle sources and the geotectonic environment of the investigated samples (Figs. 7, 8 and 9). The Type 1 is akin to the boninitic rocks and characterized by highly depletion in HFSEs and REEs relative to N-MORB. The comparison of this sample with a boninite from the Mariana arc basin (Pearce et al., 1992) displays similar enrichment pattern (Fig. 7a). The HFSE depletion may be related to retention of minor residual phases (e.g., zircon and titanite; Dixon and Batiza, 1979), re-melting of previously depleted mantle source (Green, 1973; Duncan and Green, 1987; Crawford et al., 1989) or a high degree of partial melting (Pearce and Norry, 1979). In addition, the Type 1 has lower Ti (0.19 wt%) and V (279 ppm) contents than the other samples, which is consistent with a subduction related arc setting (Fig. 8a; Shervais, 1982). The Zr/Y vs. Nb/Y and MORB-normalized Zr (M) vs Zr/Nb ratios may provide significant informations on the mantle sources (Fig. 9; Sayit et al., 2016). In particular, higher Zr/Y and Nb/Y ratios may indicate generation from an enriched mantle source (e.g., OIB; Zr/Y = 9.65 and Nb/Y = 1.65; Sun and McDonough, 1989), whereas the lower Zr/Y and Nb/Y ratios may suggest a depleted mantle source (N-MORB Zr/Y = 2.64; Nb/Y = 0.08; Sun and McDonough, 1989). The Type 1 has distinct Zr/Y ratio (0.57) compared to the arc and back-arc tectonic environments (Fig. 9a). Moreover, the MORB-normalized Zr (M) (0.079) and Zr/Nb ratio (5.36) values are remarkably lower than the back-arc and MORB environments (Fig. 9b). Therefore, the geochemical characteristics of the Type 1 clearly exhibit its boninitic nature.

The second type (Type 2) is largely akin to back arc basin basalts (BABB) and generally shows N-MORB-like HFSEs and REEs patterns coupled with negative Nb anomalies. It is known that Nb anomalies can be observed in a subduction zone because of its low solubility in acqueous fluids (Keppler, 2017) and the retention of this element by Ti-rich mineral phases (Pearce et al., 2005). The Type 2 displays trace element patterns similar to the samples from the Mariana Arc (Pearce et al., 2005) and other Neotethyan sutures (e.g., Refahiye and Karadağ regions, North-East Turkey, Parlak et al., 2013; Stepanavan and Vedi regions, Armenia, Galoyan et al., 2007; Rolland et al., 2009; Hassig et al., 2013). Also, they fall in the island arc and N-MORB fields considering their trace element systematics (Figs. 8a, b, c) which also supports the derivation within an arc-back arc setting (Shervais, 1982; Wood, 1980; Meschede, 1986). In addition, the Zr/Y ratio (2.46-2.85) vs. Nb/Y ratio (0.032-0.066) and Zr (MORB-normalized; Zr (M); 0.65-1.60) vs. Zr/Nb ratio (41.41-84.72) are consistent with the arc-back arc environments (Mariana back arc and South Sandwich island arc; Fig. 9; Table 1). All these results indicate that the Type 2 may have been derived from a subduction-modified mantle source.

The Type 3 is relatively similar to the back arc setting (Figs. 7c, 8); however it lacks the marked negative Nb anomaly and can be ascribed to the N-MORB setting. Other differences include higher Nb/Y (0.1) and lower Zr/Nb (33.0) values compared to the Type 2 (Figs. 9a, b). Overall, trace elements systematics of the magmatic rocks from the OPOZ has significant geochemical similarities with those from the Mariana back arc and the other Neotethyan sutures.

Melting systematics

The Sm/Yb vs. Dy/Yb partial melting diagram of Sayit et al. (2016) was used to understand the melting systematics of the mafic rocks from the OPOZ (Fig. 10). The samples which have higher than 4 wt% MgO concentrations (except for OV-6 = 2.97 wt% and OV-7 = 2.87 wt%), were considered for this diagram in order to avoid the effects of fractional crystallization as much as possible. High Sm/Yb ratios may indicate derivation from a garnet-bearing mantle source since the HREEs are strongly compatible in garnet. Thus, melts produced from a garnet-bearing mantle source can display strong depletion in HREE compared to LREE (Wilson, 1989; McKenzie and O'Nions, 1991). The Type 1 (boninite) has Sm/Yb = 0.39 and Dy/Yb = 1.33, testifying the highest degree of partial melting (over 30%, Fig. 10); such extremely high degrees of partial melting may be attained by re-melting of a previously depleted mantle source (Duncan and Green, 1987; Crawford et al., 1989; Çimen et al., 2016a). The Type 2 (Sm/Yb = 0.68-1.20; Dy/Yb = 1.23-2.02) may have been formed by mixing of melts deriving from garnet and spinel peridotite sources. This result is supported by nearly flat HREE patterns (Fig. 7b, c). While the Type 2 (except for PL-3) require lower degree (2-12%) of partial melting than the Type 1, the Type 3 (Sm/Yb = 1.67; Dy/Yb = 2.83) has been formed at the lowest degree of partial melting (ca. 6.5%, Fig. 10). Of note, the Type 3 is plotting far away from both melting curves and this may be tentatively attributed to the role of previous melt extraction or metasomatic processes (Sayit et al., 2016). Also, it is well-known that the H_2O-rich fluids control the degree of melting (Taylor and Martinez, 2003; Langmuir et al., 2006). Here, different water inputs derived from the subduction zone can be the main reason of the different degrees of partial melting shown by the investigated samples.
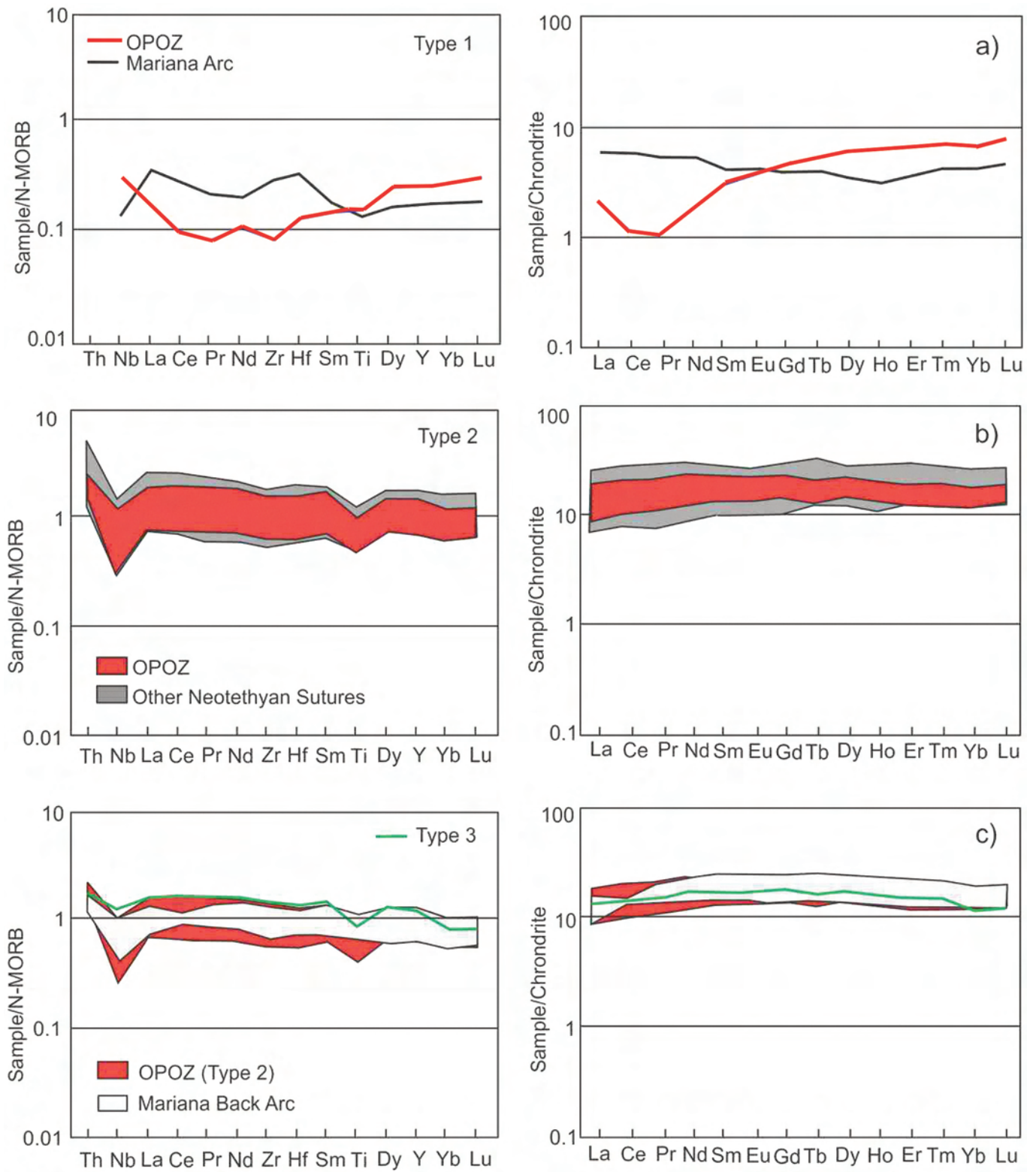
Fig. 7 - N-MORB normalized multi-element and Chondrite normalized REE spider diagrams (Sun and McDonugh, 1989). Mariana Arc-Back Arc data taken from Pearce et al. (1992), Pearce et al. (2005); Refahiye and Karadağ data taken from Parlak et al. (2013); Stepanavan and Vedi data taken from Galoyan et al. (2007); Rolland et al. (2009); Hassig et al. (2013) for the other Neotethyan Sutures.
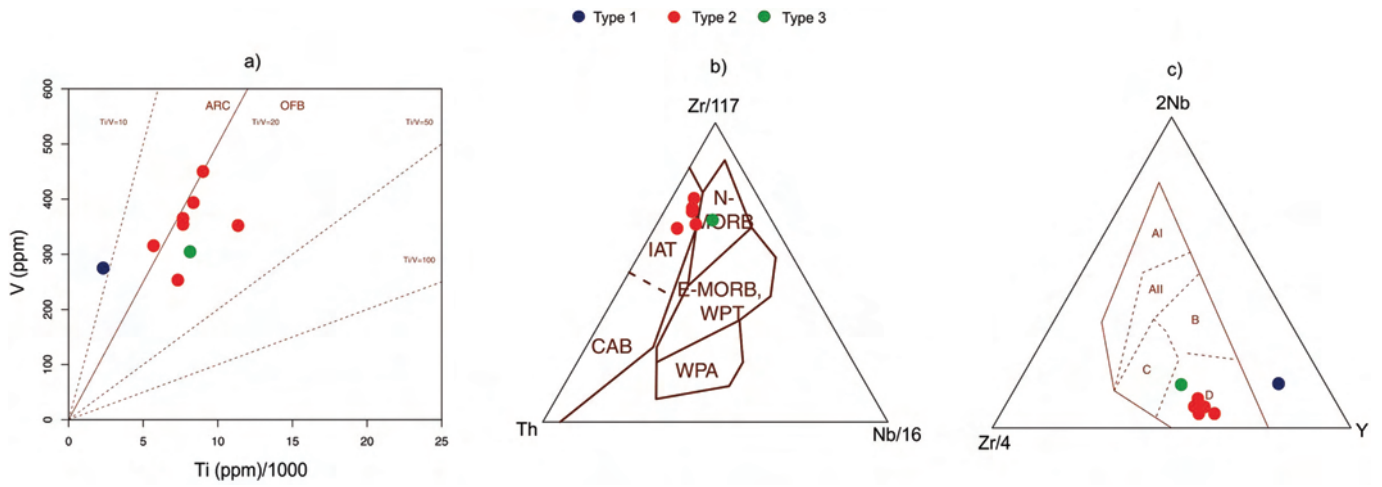
Fig. 8 - Geotectonic discrimination diagrams a) after Shervais (1982); b) after Wood (1980); c) after Meschede 1986 (AI- within-plate alkali basalt; AII- within-plate tholeiite; B- E-MORB; C and D- volcanic arc basalts; D- N-MORB).
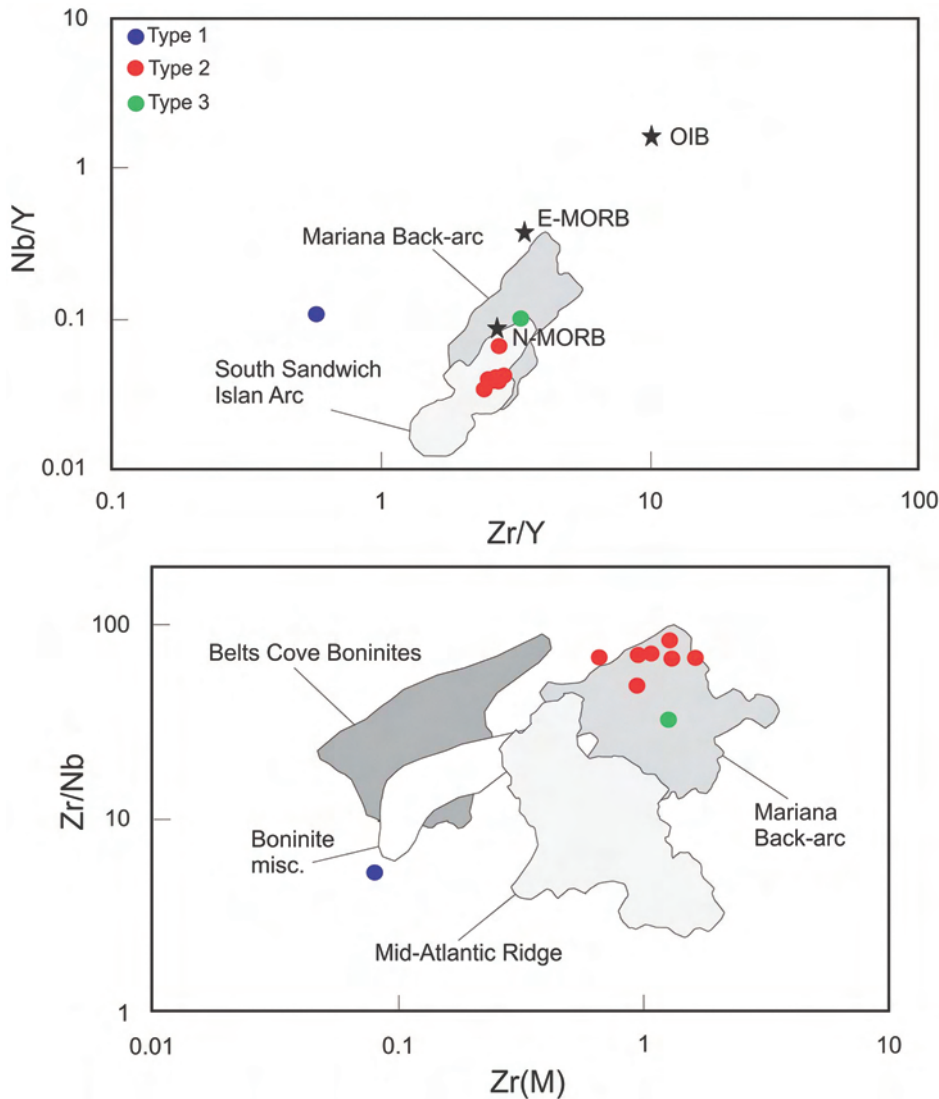
Fig. 9 - a) Zr/Y-Nb/Y and b) Zr(M)-Zr/Nb diagrams (Sayit et al., 2016). Average OIB, E-MORB and N-MORB values taken from Sun and McDonough (1989); Mariana Back-arc data taken from Pearce et al. (2005); South Sandwich Arc data taken from Pearce et al. (1995); Mid-Atlantic Ridge data taken from Niu et al. (2001); Miscellaneous boninite data taken from Cameron et al. (1983); Betts Cove boninites taken from Bedard (1999).
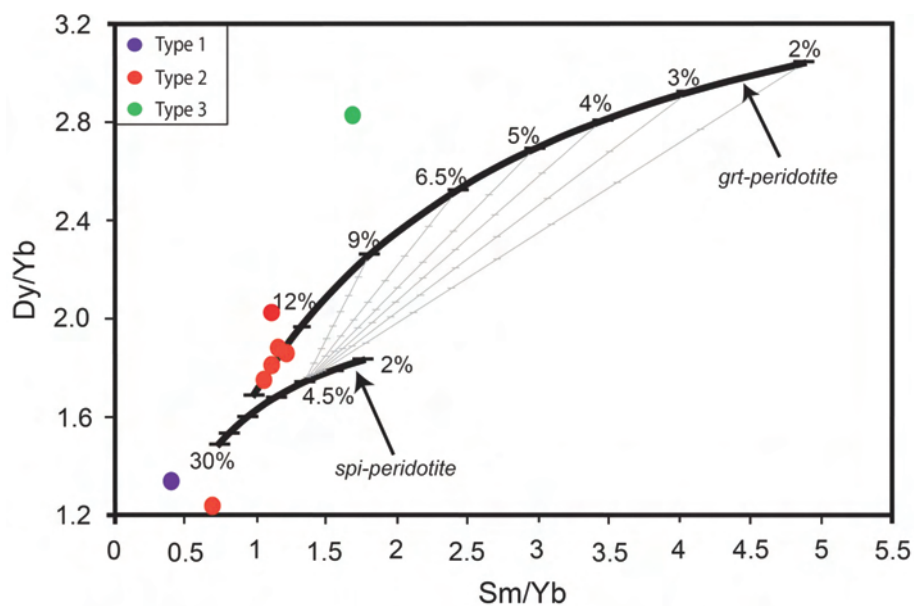
Fig. 10 - Sm/Yb-Dy/Yb partial melting model
(after Sayit et al., 2016).

An overall approach to the geodynamic evolution

The petrological characteristics of the ophiolites may provide useful information in relation to geodynamic evolution of the oceanic lithosphere (Zaccarini et al., 2011; Montanini et al., 2012; Saccani and Tassinari, 2015; Sanfilippo et al., 2015; Çimen et al., 2016b). For instance, the supra-subduction zone (SSZ) ophiolites which geochemically display island arc, fore-arc and back-arc basin signatures, represent oceanic lithosphere formed in the extended upper plates of subduction zones (Dilek and Furnes, 2014).

In Turkey, the IAESASB contains ophiolites and related mélanges including several types of magmatic rocks. The geochemical features of these rocks indicate the generation within an arc-back arc basin (e.g., Göncüoğlu et al., 2006; Aldanmaz et al., 2008; Parlak et al., 2013). In addition, the geochemical characteristics of the magmatic rocks from Armenia display supra-subduction related affinities (Knipper and Khain, 1980; Knipper et al, 1986). The OPOZ is also composed of magmatic rocks and mantle peridotites which

represent the less-known member of the IAESASB (Çimen et al., 2016b and this study). The overall geochemical evaluation of the magmatic rocks from the OPOZ suggests that it could have been formed within the intra-oceanic arc-back arc basin like other remnants of the northern branch of Neotethyan Ocean (Fig. 11).

CONCLUSIONS

The mafic magmatic rocks from the Ovacık and Pülümür Ophiolite Zone can be petrographically classified as basalts, diabases and gabbros. All of these rocks geochemically plot into the basalt field and the trace element systematics suggests that there are three different types such as boninitic, BABB-type and N-MORB. The comparison of the magmatic rocks from the OPOZ with those from the Mariana back arc basin indicates the deriving in an intra-oceanic arc-back arc setting.
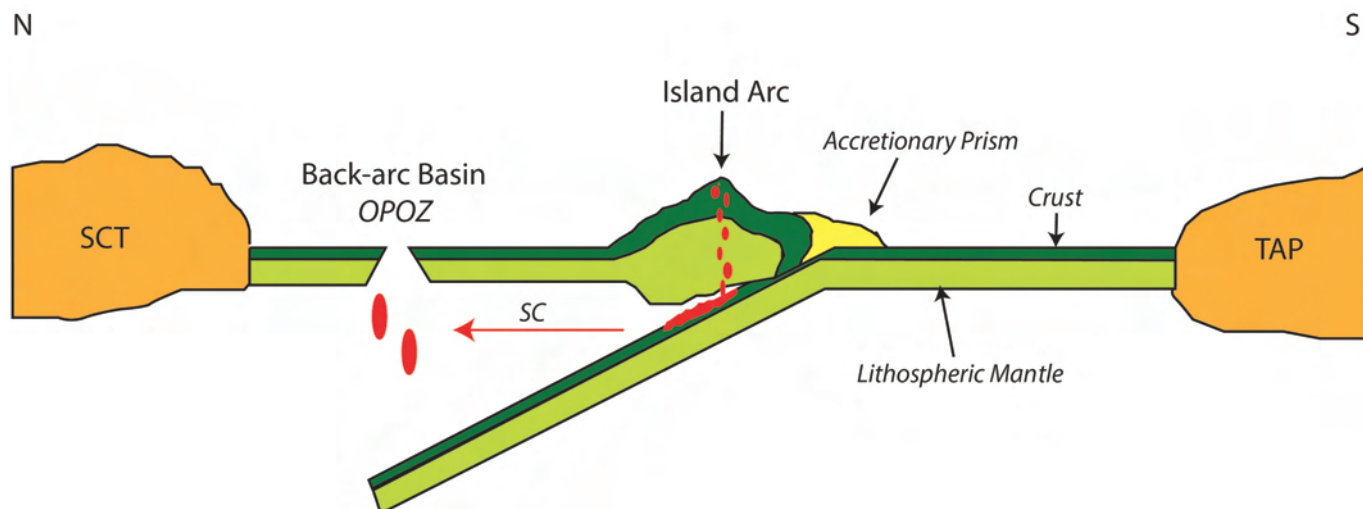

Fig. 11 - Proposed geodynamic model for generation of the OPOZ (SCT- Sakarya Composite Terrane; TAP- Tauride-Anatolide Platform).

Overall geochemical data imply that these mafic rocks were predominantly generated in a supra-subduction setting from a subduction-modified mantle source. It is further suggested that the OPOZ were formed in an oceanic arc-basin system within the northward subducting Northern Neotethys. It must be noted that the further studies are needed in order to better understand the petrological evolution of the OPOZ since this study presents the preliminary data.

ACKNOWLEDGEMENTS

REFERENCES

Akmaz R.M., Uysal I. and Saka S., 2014. Compositional variations of chromite and solid inclusions in ophiolitic chromitites from the southeastern Turkey: Implications for chromitite genesis. Ore Geol. Rev., 58: 208-224.

Aldanmaz E., Yalınız M.K., Güçtekin A. and Göncüoğlu M.C., 2008. Geochemical characteristics of mafic lavas from the Tethyan ophiolites in western Turkey: Implications for heterogeneous source contribution during variable stages of ocean crust generation. Geol. Mag., 145: 37-54.

Avagyan A., Sosson M., Philip H., Karakhanian A., Rolland Y., Melkonya R., Rebai S. and Davtyan V., 2005. Neogene to Quaternary stress field evolution in Lesser Caucasus and adjacent regions using fault kinematics analysis and volcanic cluster data. Geodyn. Acta., 18 (6): 401-4016.

Bağcı U., Parlak O. and Höck V., 2006. Geochemical character and tectonic environment of ultramafic to mafic cumulate rocks from the Tekirova (Antalya) ophiolite (Southern Turkey). Geol. J., 41: 193-219.

Bağcı U., Parlak O. and Höck V., 2008. Geochemistry and tectonic environment of diverse magma generations forming the crustal units of the Kızıldağ (Hatay) Ophiolite, Southern Turkey. Turk. J. Earth Sci., 17: 43-71.

Bedard J.H., 1999. Petrogenesis of boninites from the Betts Cove Ophiolite, Newfoundland, Canada: identification of subducted source components. J. Petrol., 40: 1853-1889.

Bortolotti V., Chiari M., Marroni M., Pandolfi L., Principi G. and Saccani E., 2013. Geodynamic evolution of ophiolites from Albania and Greece (Dinaric-Hellenic Belt): one, two or more oceanic basins? Int. J. Earth Sci., 102: 783-811.

Bozkurt E. and Oberhansli R., 2001. Menderes Massif (Western Turkey): structural, metamorphic and magmatic evolution - A synthesis. Int. J. Earth Sci., 89: 679-708.

Cameron W.E., Culloch M.T. and Walker D.A., 1983. Boninite petrogenesis: chemical and Nd-Sr isotopic constraints. Earth Planet. Sci. Lett., 65: 75-89.

Candan O., Akal C., Koralay O.E., Okay A.I., Oberhansli R., Prelevic D. and Mertz-Kraus R., 2016. Carboniferous granites on the northern margin of Gondwana, Anatolide-Tauride Block, Turkey - Evidence for southward subduction of Paleotethys. Tectonophysics, 683: 349-366.

Candan O., Çetinkaplan M., Oberhansli R., Rimmele G. and Akal C., 2005. Alpine high-pressure/low temperature metamorphism of Afyon Zone and implication for metamorphic evolution of western Anatolia, Turkey. Lithos, 84: 102-124.

Catanzariti R., Ellero A., Göncüoğlu M.C., Marroni M., Ottria G. and Pandolfi L., 2013. The Taraklı Flysch in the Boyali area (Sakarya Terrane, northern Turkey): Implications for the tec-
tonic history of the Intra-Pontide suture zone. C. R. Geosci., 345: 454-461.

Crawford A.J., Falloon T.J. and Green D.H., 1989. Classification, petrogenesis and tectonic setting of boninites. In: A.J. Crawford (Ed., Boninites. Unwin Hyman, London, p. 1-49.

Çelik Ö.F., Marzoli A., Marschik R., Chiaradia M., Neubauer F. and Öz İ., 2011. Early-Middle Jurassic intra-oceanic subduction in the İzmir-Ankara-Erzincan Ocean, Northern Turkey. Tectonophysics, 509: 120-134.

Çimen O., Göncüoğlu M.C. and Sayit K., 2016a. Geochemistry of the meta-volcanic rocks from the Çangaldağ Complex in Central Pontides: Implications for the Middle Jurassic arc - back-arc system in the Neotethyan Intra-Pontide Ocean. Turk. J. Earth Sci., 25: 491-512.

Çimen O., Göncüoğlu M.C., Simonetti A. and Sayit K., 2017. Whole rock geochemistry, Zircon U-Pb and Hf isotope systematics of the Çangaldağ Pluton: Evidences for Middle Jurassic continental arc magmatism in the Central Pontides, Turkey. Lithos, 288-289C: 35-54.

Çimen O., Toksoy Köksal F., Öztüfekçi Önal A. and Aktağ, A., 2016b. Depleted to refertilized mantle peridotites hosting chromitites within the Tunceli Ophiolite, Eastern Anatolia (Turkey): Insights on the back arc origin. Ofioliti, 41: 1-20.

Dilek Y. and Furnes H., 2014. Ophiolites and their origins. Elements, 10: 93-100.

Dilek Y. and Thy P., 2006. Age and petrogenesis of plagiogranite intrusion in the Ankara Mélange, central Turkey. Isl. Arc, 15: 44-57.

Dixon T.H. and Batiza R., 1979. Petrology and chemistry of recent lavas in the Northern Marianas: Implications for the origin of island arc basalts. Contrib. Mineral. Petrol., 70: 167-181.

Duncan R.A. and Green D.H., 1987. The genesis of refractory melts in the formation of oceanic crust. Contrib. Mineral. Petrol., 96: 326-342.

Ellero A., Ottria G., Sayit K., Catanzariti R., Frassi C., Göncüoğlu M.C., Marroni M. and Pandolfi L., 2015. Geological and geochemical evidence for a Late Cretaceous continental arc in the central Pontides, northern Turkey. Ofioliti, 40: 73-90.

Eyüboğlu Y., Bektas O. and Pul D., 2007. Mid-Cretaceous olistostromal ophiolitic mélange developed in the back-arc basin of the eastern pontide magmatic arc, Northeast Turkey. Int. Geol. Rev., 49: 1103-1126.

Floyd P.A., 1993. Geochemical discrimination and petrogenesis of alkalic basalt sequences in part of the Ankara Mélange, central Turkey. J. Geol. Soc. London, 150: 541-550.

Floyd P.A. and Winchester J.A., 1978. Identification and discrimination of altered and metamorphosed volcanic rocks using immobile elements. Chem. Geol., 21: 291-306.

Floyd P.A., Winchester J.A., Seston R., Kryza R. and Crowley Q.G., 2000. Review of geochemical variation in Lower Palaeozoic metabasites from the NE Bohemian Massif; intracratonic rifting and plume ridge interaction. In: W. Franke, V. Haak, O. Oncken and D. Tanner (Eds.), Orogenic processes: Quantifications and modeling in the Variscan Belt. Geol. Soc. London Spec. Publ., 179: 155-174.

Frassi C., Göncüoğlu M.C., Marroni M., Pandolfi L., Ruffini L., Ellero A., Ottria G. and Sayit, K., 2016. The Intra-Pontide suture zone in the Tosya-Kastamonu area, Northern Turkey. J Maps., 1: 211-219.

Galoyan G., Rolland Y., Sosson M., Corsini M. and Melkonyan, R., 2007. Evidence for superposed MORB, oceanic plateau and volcanic arc series in the Lesser Caucasus (Stepanavan, Armenia). C.R. Geosci., 339: 482-492.

Galoyan G., Rolland Y., Sosson M., Corsini M., Billo S., Verati C. and Melkonyan R., 2009. Geology, geochemistry and $^{40}Ar/^{39}Ar$ dating of Sevan ophiolites (Lesser Caucasus, Armenia): Evidence for Jurassic back-arc opening and hot spot event between the South Armenian block and Eurasia. J Asian Earth Sci., 34: 135-153.

Göncüoğlu M.C., 2010. Introduction to the geology of Turkey: Geodynamic evolution of the pre-Alpine and Alpine Terranes. MTA., p. 1-69.

Göncüoğlu M.C., Kozlu H. and Dirik K., 1997. Pre-Alpine and Alpine terranes in Turkey: Explanatory notes to the terrane map of Turkey. Ann. Géol. Pays. Hellén., 37: 515-536.

Göncüoğlu M.C., Marroni M., Pandolfi L., Ellero A., Ottria G., Catanzariti R., Tekin U.K. and Sayit K., 2014. The Arkot Dağ Mélange in Araç area, central Turkey: Evidence of its origin within the geodynamic evolution of the Intra-Pontide suture zone. J Asian Earth Sci., 85: 117-139.

Göncüoğlu M.C., Turhan N., Sentürk K., Özcan A. and Uysal S., 2000. A geotraverse across NW Turkey: tectonic units of the Central Sakarya region and their tectonic evolution. In: E. Bozkurt, J.A. Winchester and J.D. Piper (Eds.), Tectonics and magmatism in Turkey and the surrounding Area. Geol. Soc. London Spec. Publ., 173: 139-162.

Göncüoğlu M.C., Yalınız M.K. and Tekin U.K., 2006. Geochemistry, tectono-magmatic discrimination and radiolarian ages of basic extrusives within the Izmir-Ankara Suture Belt (NW Turkey): Time constraints for the Neotethyan evolution. Ofioliti, 31: 25-38.

Green D.H., 1973. Experimental nelting studies on a model upper mantle composition at high pressure under watersaturated and water-unsaturated conditions. Earth Planet. Sci. Lett., 19: 37-53.

Hässig M., Rolland Y., Sosson M., Galoyan G., Sahakyan L., Topuz G., Çelik Ö.F., Avagyan A. and Müller C., 2013. Linking the NE Anatolian and Lesser Caucasus ophiolites: Evidence for large-scale obduction of oceanic crust and implications for the formation of the Lesser Caucasus-Pontides Arc. Geodyn Acta., 26 (3-4): 311-330.

Janoušek V., Farrow C.M. and Erban V., 2006. Interpretation of whole-rock geochemical data in igneous geochemistry: Introducing Geochemical Data Toolkit (GCDkit). J Petrol., 47: 1255-1259.

Keppler H., 2017. Fluids and trace element transport in subduction zones. Am. Mineral., 102: 5-20.

Knipper A.L. and Khain E.V., 1980. Structural position of ophiolites of the Caucasus. In: G. Rocci (Ed.), Tethyan Ophiolites, Vol.2 Eastern Area. Special Issue: 297-314.

Knipper A.L., Ricou L.E. and Dercourt J., 1986. Ophiolites as indicators of the geodynamic evolution of the Tethyan ocean. Tectonophysics, 123: 213-240.

Langmuir C.H., Bézos A., Escrig S. and Parman S.W., 2006. Chemical systematics and hydrous melting of the mantle in back-arc basins. In: D.M. Christie, C.R. Fisher, S. Lee and S. Givens. (Eds.), Back-arc spreading systems: Geological, biological, chemical and physical interactions. Geoph. Monogr. Series, 166: 87-146.

Marroni M., Frassi C., Göncüoğlu M.C., Di Vincenzo G., Pandolfi L., Rebay G., Ellero A. and Ottaria G., 2014. Late Jurassic amphibolite-facies metamorphism in the Intra-Pontide Suture Zone (Turkey): an eastward extension of the Vardar Ocean from the Balkans into Anatolia? J Geol. Soc, London, 171: 605-608.

McKenzie D. and O'Nions R.K., 1991. Partial melt distributions from inversion of rare earth element concentrations. J. Petrol., 32: 1021-1091.

McKenzie D. and O'Nions R.K., 1995. The source regions of ocean island basalts. J. Petrol., 36:133-159.

Meschede M., 1986. A method of discriminating between different types of midocean ridge basalts and continental tholeiites with the Nb-Zr-Y diagram. Chem. Geol., 56: 207-218.

MTA (Mineral Research and Exploration General Directorate), 2008. Geol. Rep. J42-J43.

Montanini A. and Tribuzio L., 2001. Gabbro-derived granulites from the Northern Apennines (Italy): Evidence for lower-crustal emplacement of tholeiitic liquids in post-Variscan times. J. Petrol., 42: 2259-2277.

Montanini A., Tribuzio L. and Thirlwall M., 2012. Garnet clinopyroxenite layer from the mantle sequence of the Northern Apennine ophiolites (Italy): Evidence for recycling of crustal material. Earth. Planet. Sci. Lett., 351-352: 171-181.

Niu Y., Bideau D., Hekinian R. and Batiza R., 2001. Mantle compositional control on the extent of mantle melting, crust production, gravity anomaly, ridge morphology, and ridge segmentation: A case study at the Mid-Atlantic Ridge 33-35°. Earth Planet. Sci. Lett., 186: 383-399.

Okay A.I., 2008. Geology of Turkey: Synopsis. Anschnitt., 21: 19-42.

Okay A.I. and Sahintürk Ö., 1997. Geology of the Eastern Pontides, In: A.G. Robinson (Ed.), Regional and petroleum geology of the Black Sea and surrounding region: Am. Ass. Petrol. Geol. Mem., 68: 291-311.

Önen P. and Hall R., 1993. Ophiolites and related metamorphic rocks from the Kütahya region, northwest Turkey. Geol. J., 28: 399-412.

Özgül N., 1984. Stratigraphy and tectonic evolution of the Central Taurides. In: O. Tekeli and M.C. Göncüoğlu (Eds.), Geology of Taurus Belt., MTA, p. 77-90.

Özgül N., Turşucu A., Özyardımcı N., Şenol M., Bingöl İ. and Uysal Ş., 1981. Munzur Dağlarının jeolojisi. MTA Rapor No: 6995, Ankara (unpublished - in Turkish).

Parlak O., 2016. The tauride ophiolites of Anatolia (Turkey): A review. J Earth Sci., 27 (6): 901-934.

Parlak O., Çolakoğlu A., Dönmez C., Sayak H., Yıldırım N., Türkel A. and Odabaşı İ., 2013. Geochemistry and tectonic significance of ophiolites along the Ankara-Erzincan Suture Zone in northeastern Anatolia. In: A.H.F. Robertson, O. Parlak and U.C. Ünlügenç (Eds.), Geol. Soc. London Spec. Publ., 372: 75-105.

Pearce J.A., 1996. A user guide to basalt discrimination diagrams. In: D.A. Wyman (Ed.), Trace element geochemistry of volcanic rocks: Applications for massive sulphide exploration. Short Course Notes 12. St. John's, Canada. Geol. Ass. Can., p. 79-113.

Pearce J.A. and Cann J.R., 1973. Tectonic setting of basic volcanic rocks determined using trace element analyses. Earth Planet. Sci. Lett., 19 (2): 290-300.

Pearce J.A. and Norry M., 1979. Petrogenetic implications of Ti, Zr, Y and Nb variations in volcanic rocks. Contrib Mineral. Petrol., 69: 33-47.

Pearce J.A., Ernewein M., Bloomer S.H., Parson L.M., Murton B.J. and Johnson L.E., 1995. Geochemistry of Lau Basin volcanic rocks: influence of ridge segmentation and arc proximity. In: J.L. Smellie (Ed.), Volcanism associated with extension at consuming plate margins. Geol. Soc. London Spec. Publ., 81: 53-75.

Pearce J.A., Stern R.J., Bloomer S.H. and Fryer P., 2005. Geochemical mapping of the Mariana arc-basin system: Implications for the nature and distribution of subduction components. Geochem Geophys., 6: 1-27.

Pearce J.A., Van der Laan S.R., Arculus R.J., Murton B.J., Ishii T., Peate D.W. and Parkinson I.J., 1992. Boninite and harzburgite from Leg 125 (Bonin-Mariana forearc): A case study of magma genesis during the initial stages of subduction. Proc. O. D. P. Sci Res., 125: 623-659.

Rice S.P., Robertson A.H.F. and Ustaömer T., 2006. Late Cretaceous-Early Cenozoic tectonic evolution of the Eurasian active margin in the Central and Eastern Pontides, northern Turkey. In: A.H.F. Robertson (Ed.), Tectonic development of the Eastern Mediterranean region. Geol. Soc. London Spec. Publ., 260: 413-445.

Robertson A.H.F., 2002. Overview of the genesis and emplacement of Mesozoic ophiolites in the Eastern Mediterranean Tethyan region. Lithos, 65: 1-67.

Robertson A.H.F., Parlak O., Ustaömer T., Taslı K., İnan N., Dumitrica P. and Karaoğlan F., 2014. Subduction, ophiolite genesis and collision history of Tethys adjacent to the Eurasian continental margin: New evidence from the Eastern Pontides, Turkey. Geodyn. Acta, 1-64.

Rolland Y., Galoyan Gh., Bosch D., Sosson M., Corsini M., Fornari M. and Vérati C., 2009. Jurassic back-arc and Cretaceous hot-spot series in the Armenian ophiolites - Implications for the obduction process. Lithos, 112: 163-187.

116

Rolland Y., Galoyan G., Sosson M., Melkonian R. and Avagyan A., 2010. The Armenian ophiolite: Insights for Jurassic back-arc formation, Lower Cretaceous hot spot magmatism and Upper Cretaceous obduction over the South Armenian block. In M. Sosson, R.A. Stephenson, F. Bergerat and V. Starostenko (Eds.), Sedimentary basin tectonics from the Black Sea and Caucasus to the Arabian Platform. Geol. Soc. London Spec. Publ., 340: 353-382.

Saccani E. and Tassinari R., 2015. The role and MORB and SSZ magma-types in the formation of Jurassic ultramafic cumulates in the Mırdıta Ophiolites (Albania) as deduced from chromian spinel and olivine e chemistry. Ofioliti, 40 (1): 37-56.

Sanfilippo A., Tribuzio R., Tiepolo M. and Berno D., 2015. Reactive flow as dominant evolution process in the lowermost oceanic crust: evidence from olivine of the Pineto ophiolite (Corsica). Contrib. Mineral. Petrol., 170 (38): 1-12.

Sayit K., Marroni M., Göncüoğlu M.C., Pandolfi L., Ellero A., Ottria G. and Frassi C., 2016. Geological setting and geochemical signatures of the mafic rocks from the Intra-Pontide Suture Zone: implications for the geodynamic reconstruction of the Mesozoic Neotethys. In. J. Earth Sci., 105: 39-64.

Shervais J.W., 1982. Ti-V plots and the petrogenesis of modern ophiolitic lavas. Earth Planet. Sci. Lett., 59: 101-118.

Sun S.S. and McDonough W.F., 1989. Chemical and isotopic systematics of oceanic basalts: implications for mantle composition and processes. Geol. Soc. London Spec. Publ., 42: 313-345.

Şengör A.M.C. and Yılmaz Y., 1981. Tethyan evolution of Turkey: A plate tectonic approach. Tectonophysics, 75: 181-241.

Taylor B. and Martinez F., 2003. Back-arc basin basalt systematics. Earth Planet. Sci. Lett., 210: 481-497.

Topuz G., Çelik O.F., Şengör A.M.C., Altıntaş I.E., Zack T., Rolland Y. and Barth M., 2013. Jurassic ophiolite formation and emplacement as backstop to a subduction-accretion complex in northeast Turkey, the Refahiye ophiolite, and relation to the Balkan ophiolites. Am. J. Sci., 313: 1054-1087.

Uysal İ., Ersoy E.Y., Dilek Y., Escaloya M., Sarıfakıoğlu E., Saka S. and Hirata T., 2015. Depletion and refertilization of the Tethyan oceanic upper mantle as revealed by the Early Jurassic Refahiye ophiolite, NE Anatolia-Turkey. Gondw. Res., 27: 594-611.

Uysal İ., Zaccarini F., Garuti G., Meisel T., Tarkian M., Bernhardt H.J. and Sadıklar M.B., 2007. Ophiolitic chromitites from the Kahramanmaraş area, southeastern Turkey: their platinumgroup elements (PGE) geochemistry, mineralogy and Os-isotope signature. Ofioliti, 32: 151-161.

Wilson B.M., 1989. Igneous petrogenesis: A global tectonic approach. London, UK, Unwin Hyman. 466 pp.

Wood D.A., 1980. The application of a Th-Hf-Ta diagram to problems of tectonomagmatic classification and to establishing the nature of crustal contamination of basaltic lavas on the British Tertiary Volcanic Province. Earth Planet Sci Lett., 50: 11-30.

Wood D.A., Gibson I.L. and Thompson R.N., 1976. Elemental mobility during zeolite facies metamorphism of the Tertiary basalts of eastern Iceland. Contrib Mineral Petrol., 55: 241-254.

Yalınız M.K., Floyd P.A. and Göncüoğlu M.C., 2000. Geochemistry of volcanic rocks from the Çiçekdağı ophiolite, central Anatolia, Turkey, and their inferred tectonic setting within the Northern branch of the Neotethyan ocean. In: E. Bozkurt, J.A. Winchester and J.D.A. Piper (Eds.), Tectonics and magmatism in Turkey and the surrounding area. Geol. Soc. London Spec. Publ., 173: 171-182.

Yılmaz A. and Yılmaz H., 2013. Ophiolites and ophiolitic mélanges of Turkey: A eview. Geol. Bull. Turk., 56 (2): 61-114.

Yılmaz Y., Tüysüz O., Yiğitnaş E., Genc C.S.and Şengör A.M.C., 1997. Geology and tectonic evolution of the Pontides. In: A.G. Robinson (Ed.), Regional and petroleum geology of the Black Sea and surrounding region. Am. Ass. Petr. Geol. Mem., 68: 183-226.

Zaccarini F., Garuti G., Proenza J.A., Campos L., Thalhammer O.A.R., Aiglsperger T. and Lewis J., 2011. Chromite and platinum-group-elements mineralization in the Santa Elena ophiolitic ultramafic nappe (Costa Rica): Geodynamic implications. Geol. Acta, 9 (3): 407-423.